

Density screening effects in the NJL model: Chiral condensate, speed of sound, and the Critical End Point

A. Rosas Díaz¹, A. Raya Montaña^{2,3}, C. A. Vaquera Araujo⁴,
and S. Hernández-Ortiz^{2,5}

¹Instituto de Física y Matemáticas, Universidad Michoacana
de San Nicolás de Hidalgo, México

²Facultad de Ingeniería Eléctrica, Universidad Michoacana de
San Nicolás de Hidalgo, México

³Centro de Ciencias Exactas, Universidad del Bío-Bío. Chile

⁴División de Ciencias e Ingenierías, Universidad de
Guanajuato

⁵Universidad Aeronáutica en Queretaro, México

March, 2026

Abstract

The phase diagram of Quantum Chromodynamics (QCD) remains a central topic in high-energy physics. At high temperature and low baryochemical potential, the chiral transition is experimentally observed and theoretically explored to be a smooth crossover, while at high densities, a first-order phase transition is theoretically expected in lack of direct experimental evidence. The search for the Critical End Point (CEP), where both regimes meet, is one of the main objectives of heavy-ion experiments at FAIR and NICA. In this work, we explore the QCD phase diagram structure using the Nambu–Jona-Lasinio (NJL) model, incorporating medium screening effects through an effective coupling $G(T, \mu)$ for $\mu \gg T \sim 0$. We apply a consistent regularization scheme and Sommerfeld expansion to include low thermal and large density corrections in the gap equation. Our numerical

analysis focuses on the behavior of the chiral condensate, the dynamical quark mass, and the speed of sound. We find that screening effects shift the possible position of the CEP and modify the nature of the chiral transition. These findings provide theoretical support for ongoing experimental searches and may have implications for the physics of compact stars.

1 Introduction

Understanding the phase structure of Quantum Chromodynamics (QCD) under extreme conditions remains a central challenge in modern high-energy physics [1, 2]. Lattice QCD calculations have established that, at vanishing baryochemical potential, the transition from hadronic matter to the quark–gluon plasma (QGP) is a smooth crossover [3, 4, 5]. However, the notorious sign problem prevents a reliable *ab initio* determination of the phase diagram at large baryon density [6, 7], leaving open fundamental questions about the existence and location of a possible Critical End Point (CEP) and the order of the chiral transition at high baryochemical potential [8]. Experimental programs such as the Beam Energy Scan at RHIC and upcoming measurements at FAIR and NICA aim to search for experimental signatures of the CEP [9, 10], motivating parallel theoretical studies using effective approaches that can access the high-density, low-temperature regime.

Effective models that capture the chiral dynamics of QCD, notably the Nambu–Jona-Lasinio (NJL) model, remain indispensable tools for exploring qualitative and semi-quantitative features of the QCD phase diagram [11, 12, 13]. The NJL framework successfully describes spontaneous chiral symmetry breaking and the associated low-energy meson phenomenology while being sufficiently simple to allow controlled studies of medium effects [12, 13, 14]. A common assumption in many NJL analyses is the use of a constant four-fermion coupling G [15]. Yet, in a dense medium one expects screening of interactions and in-medium modification of the effective coupling: neglecting such density-dependent screening may obscure important shifts in the order of the transition and in the location of the CEP.

In this work we extend the two-flavor NJL model by incorporating medium screening effects through a density- and temperature-dependent effective coupling $G(T, \mu)$. Our aim is to assess how a physically motivated reduction of the scalar-channel attraction at large chemical potential modifies the chiral condensate, the dynamical quark mass, and bulk thermodynamic observables sensitive to the equation of state, such as the speed of sound c_s^2 [16, 17]. We treat the model in the Hartree (mean-field) approximation and solve the

resulting gap equation,

$$m = m_0 - 2G\langle\bar{\psi}\psi\rangle,$$

employing a consistent regularization prescription tailored to the nonrenormalizable nature of the NJL model. For the finite-density, low-temperature regime of interest ($\mu \gg T \sim 0$) we use the Sommerfeld expansion to include the leading thermal corrections to the medium integrals, which allows us to obtain analytic control of the dominant density-dependent contributions.

A key aspect of our study is the explicit comparison between results obtained with a constant coupling G and those obtained with the density- and temperature-dependent effective coupling $G'(T, \mu)$ that differs from $G(T, \mu)$ by including the screening corrections. While the parametrization we adopt for $G'(T, \mu)$ is phenomenological, it captures the expected weakening of the scalar attraction with increasing density and therefore isolates the qualitative impact of screening on chiral restoration. We pay special attention to the behavior of the squared of the speed of sound at constant entropy,

$$c_s^2 = \left. \frac{\partial p}{\partial \varepsilon} \right|_s,$$

which provides a sensitive probe of the stiffness of the equation of state and can display characteristic signals near phase transitions or a CEP. Our numerical analysis focuses on the dynamical mass, the chiral condensate, the baryon density and susceptibilities, and the resulting $c_s^2(\mu, T)$, identifying trends that suggest how screening shifts and modifies the nature of the chiral transition at low temperatures and large chemical potentials.

To close this introduction we provide a brief outline of the manuscript. In Sect. 2 we present the theoretical framework, define the two-flavor NJL model in the Hartree approximation, describe the regularization scheme, and derive the modified gap equation including the Sommerfeld expansion for $\mu \gg T$. In Sect. 3 we present the numerical results for the dynamical mass, the chiral condensate, the baryon density and susceptibilities, and the speed of sound, comparing the cases of constant and screened couplings and discussing the implications for the possible location and signatures of the CEP. Finally, Sect. 4 summarizes our main conclusions and outlines prospects for future work.

2 Theoretical Framework

The starting point is the two-flavor Lagrangian for light quarks with scalar and pseudoscalar interactions, which we write as

$$\mathcal{L}_{NJL} = \bar{\psi}(i\gamma^\mu\partial_\mu - m_0)\psi + G [(\bar{\psi}\psi)^2 + (\bar{\psi}i\gamma_5\vec{\tau}\psi)^2], \quad (1)$$

where ψ denotes the field of two-flavor, three-color quarks, m_0 is the bare mass, which can be small or taken to be zero in the chiral limit, $\vec{\tau}$ are the Pauli matrices acting in the two-flavor isospin space, and G is the coupling constant, [18]. The beauty of the NJL model as an effective approximation is that at low energies (Λ_{QCD} typically on the order of hundreds of MeV), the chiral condensate complies with $\langle\bar{\psi}\psi\rangle \neq 0$, since the model generates this expectation value in the non-trivial vacuum. Despite being unable to explain the phenomenon of confinement, the NJL model successfully describes the structure of light pseudoscalar mesons, such as pions or kaons [12, 14]. This is achieved through quark-antiquark bound states (in the sense of a collective state), as well as the spontaneous breaking of chiral symmetry. We employ the two-flavor NJL model in the Hartree approximation [13, 15], leading to a self-consistent gap equation for the dynamical quark mass m . In this approximation, the chiral condensate becomes

$$\langle\bar{\psi}\psi\rangle = -\text{Tr} \int \frac{d^4p}{(2\pi)^4} \frac{1}{\not{p} + m}, \quad (2)$$

and from the gap equation $m = m_0 - 2G\langle\bar{\psi}\psi\rangle$, we explicitly have that

$$m = m_0 - 2G \int \frac{d^4p}{(2\pi)^4} \text{Tr} \frac{1}{\not{p} - m}. \quad (3)$$

The well-known procedure indicated to solve this gap equation is to regularize the integral, typically by means of a cut at the Euclidean moment Λ , since the NJL model is not renormalizable, and thus obtain a transcendental equation for m [12]

$$m = m_0 + 4GN_f N_c \left[\frac{1}{(2\pi)^2} m^3 \left(\frac{1}{\epsilon} - \gamma_E \right) \right], \quad (4)$$

where the regulator $1/\epsilon$ as $\epsilon \rightarrow 0$ is related to the Λ cut-off and γ_E is the Euler-Mascheroni constant. Now, when considering a medium at a given temperature T and density parametrized by a baryochemical potential μ , the integral involved in the gap equation is no longer analytical, and one needs to evaluate

$$I_{FD} = \int_0^\infty \frac{k^2}{\sqrt{k^2 + m^2}} (n_F(\mu, T) + \bar{n}_F(\mu, T)) dk, \quad (5)$$

where,

$$n_F(\mu, T) = \frac{1}{e^{\frac{\sqrt{k^2 + m^2} - \mu}{T}} + 1}, \quad \bar{n}_F(\mu, T) = \frac{1}{e^{\frac{\sqrt{k^2 + m^2} + \mu}{T}} + 1}, \quad (6)$$

where the functions n_F and \bar{n}_F correspond to the Fermi–Dirac distributions [19]. Using $E = \sqrt{k^2 + m^2}$, we have

$$I_{FD} = \int_m^\infty \sqrt{E^2 - m^2} [n_F(E) + \bar{n}_F(E)] dE. \quad (7)$$

In the regime $\mu \gg m$ with finite T , $\bar{n}_F \approx e^{-(E+\mu)/T}$ is vanishingly small and can be discarded. Then, at the second order of the Sommerfeld expansion [20, 21], the above integral reduces to

$$I_{FD} = \int_m^\mu f(E) dE + \frac{\pi^2 T^2}{6} f'(\mu), \quad (8)$$

with

$$f(E) = \sqrt{E^2 - m^2}, \quad f'(\mu) = \frac{\mu}{\sqrt{\mu^2 - m^2}},$$

where the second term describes the thermal corrections to the system and the first term can be integrated analytically

$$\begin{aligned} I_0 &= \int_m^\mu \sqrt{E^2 - m^2} dE \\ &= \left\{ \frac{E}{2} \sqrt{E^2 - m^2} - \frac{m^2}{2} \ln[E + \sqrt{E^2 - m^2}] \right\} \Big|_m^\mu. \end{aligned} \quad (9)$$

In the upper limit $E = \mu$, we have $\sqrt{\mu^2 - m^2} \approx \mu - \frac{m^2}{2\mu}$ and $\ln[E + \sqrt{E^2 - m^2}] \approx \ln(2\mu)$. Conversely when $E = m$, $\sqrt{E^2 - m^2}$ vanishes and only the term $\sim \frac{m^2}{2} \ln(m)$ survives. Therefore,

$$I_0 = \frac{\mu}{2} \sqrt{\mu^2 - m^2} - \frac{m^2}{2} \ln \left(\frac{2\mu}{m} \right), \quad (10)$$

and for the thermal corrections,

$$\frac{\pi^2 T^2}{6} \frac{\mu}{\sqrt{\mu^2 - m^2}} \approx \frac{\pi^2 T^2}{6}. \quad (11)$$

Then, the complete integral is

$$\begin{aligned} I_{FD} &\approx \frac{\mu}{2} \sqrt{\mu^2 - m^2} - \frac{m^2}{2} \ln \left(\frac{2\mu}{m} \right) + \frac{\pi^2 T^2}{6} \\ &= \frac{\mu^2}{2} - \frac{m^2}{2} \left[\ln \left(\frac{2\mu}{m} \right) + 1 \right] + \frac{\pi^2 T^2}{6}. \end{aligned} \quad (12)$$

By neglecting terms in the high-density limit and considering the regularization scheme, the full expression for the gap equation reduces to

$$m = m_0 + 4mGN_fN_C \left[\frac{1}{(2\pi)^2} m^2 \left(\frac{1}{\epsilon} - \gamma_E \right) - \frac{\mu^2}{2} + \frac{m^2}{2} \ln \left(\frac{\mu}{m} \right) + \frac{\pi^2 T^2}{6} \right]. \quad (13)$$

3 Theoretical Framework

We proceed to solve the Eq. (13) for the dynamical mass m using different values of T and μ . Figure 1 shows the solutions to the gap equation for different temperatures. Expectedly, the dynamical effects are screened at large μ for the temperatures under consideration. Next, we explore the variations of the solutions to the gap equation when monotonically we increase the value of the current quark mass m_0 . Figure 2 shows such changes at a fixed value of μ

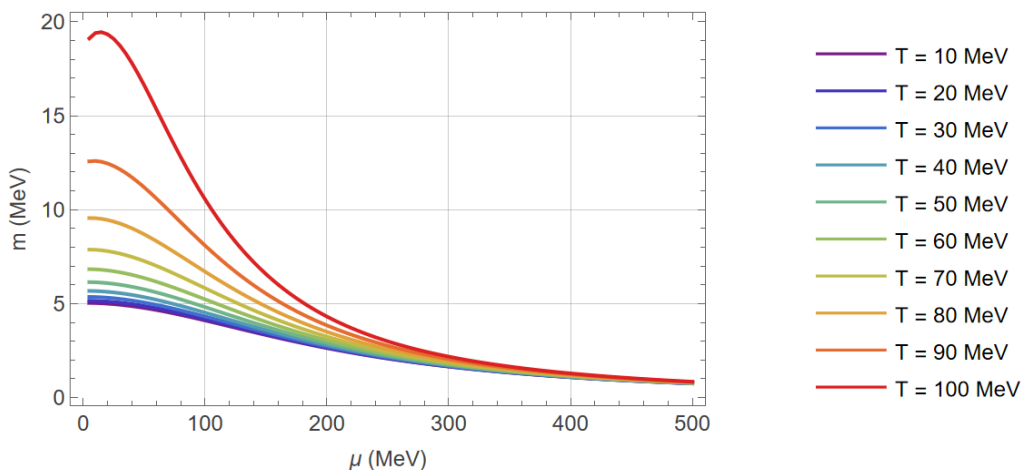


Figure 1: Solutions to the gap equation for different temperatures.

Now, because the dynamical mass is directly related to the chiral condensate $\langle \bar{\psi}\psi \rangle$, the changes in the behavior of this chiral order parameter modify other observables like the speed of sound c_s^2 , which is defined as [16]:

$$c_s^2 = \left. \frac{\partial p}{\partial \epsilon} \right|_s = \frac{n\chi_{TT} - s\chi_{\mu T}}{\mu(\chi_{TT}\chi_{\mu\mu} - \chi_{\mu T}^2)}, \quad (14)$$

where

$$n = \int \frac{\partial \langle \bar{\psi}\psi \rangle}{\partial \mu} dm_0 \quad \text{and} \quad \chi_{xy} = \frac{\partial \langle \bar{\psi}\psi \rangle}{\partial x \partial y}. \quad (15)$$

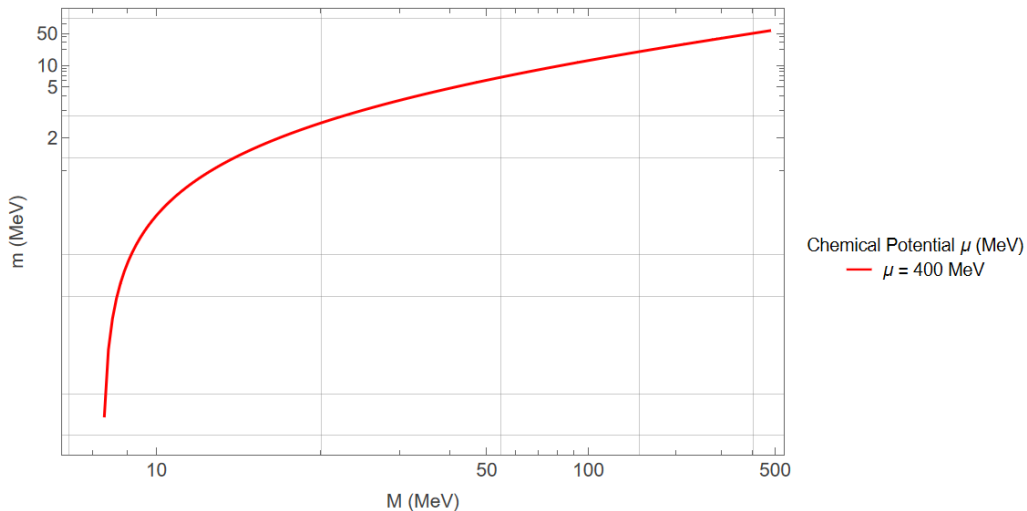


Figure 2: Dynamical mass as a function of the seed mass for fix chemical potential.

The modifications of the speed of sound at very low temperatures we be derived analytically, yielding

$$c_s^2 \approx \frac{n}{\mu} \left(\frac{\partial n}{\partial \mu} \right)^{-1}. \quad (16)$$

Figure 3 show the behavior of the density n for differents values of μ and Figure 4 show the behavior of the speed of sound c_s^2 as a function of μ . Notice that as μ grows bigger, the speed of sound reaches the conformal value.

In QCD, the conformal limit arises in the high energy regime, where the strong interactions weakens ($\alpha_s \rightarrow 0$) and QGP behaves like an ideal gas with $c_s^2 = \frac{1}{3}$ [19]. On the other hand, although QCD is not an exactly conformal theory, certain approximations such as the limit of large N_c or regimes where T and μ are very large can exhibit behavior close to conformal invariance [22]. The approximation of $c_s^2 \approx \frac{1}{3}$ at low temperatures in the NJL model reflects behavior close to the conformal limit of QCD, where the speed of sound in a relativistic fluid satisfying $c_s^2 = \frac{1}{3}$.

Finally, adding screening effects of the medium by modifying the coupling constant $G \rightarrow G' = G \frac{m'}{m}$, where m is the mass in a vacuum and m' is the mass in a medium, we obtain Fig. 5. At large densities, the NJL model behaves as a relativistic gas of free quarks, where the screening effects in G' do not alter the equation of state of the system.

For the case of fixed G the curve in Fig. 3 decreases monotonically between approximately $2.5 > n > 0$ in $\mu \leq 1000$ MeV, without crossing the negative

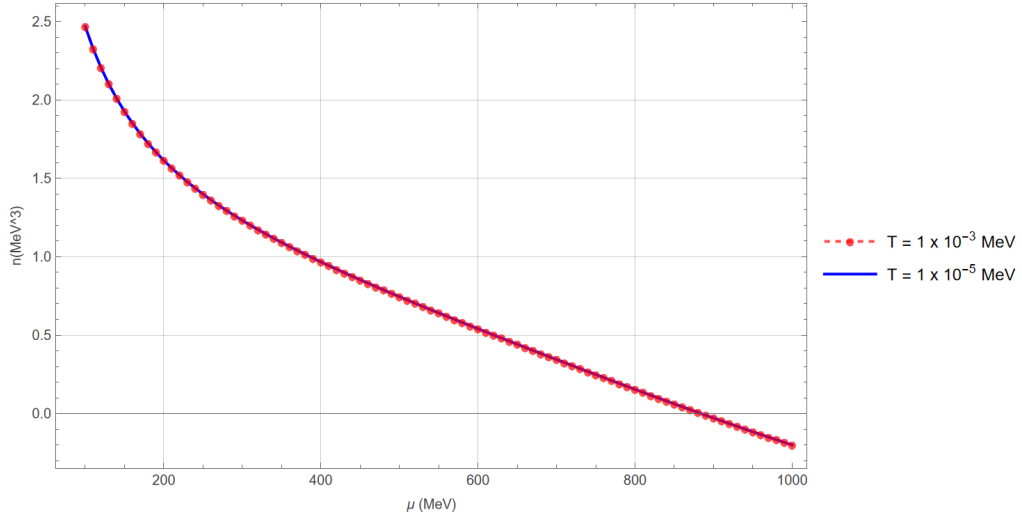


Figure 3: Calculation of the density n in the medium at low temperatures $T \approx 1 \times 10^{-3}$ MeV and 1×10^{-5} MeV

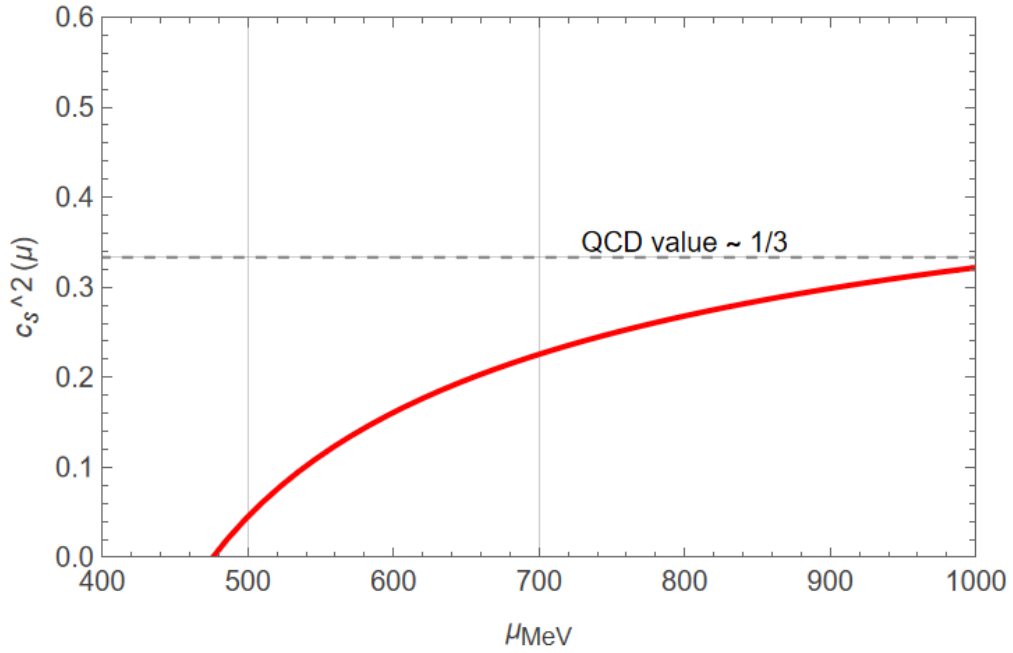


Figure 4: Calculation of the speed of sound in the medium at a low temperature $T \approx 1 \times 10^{-3}$ MeV

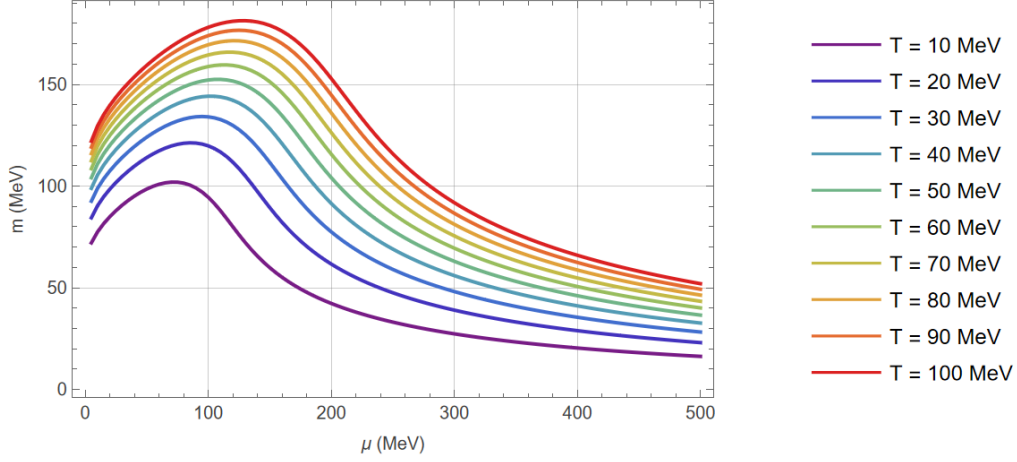


Figure 5: Gap equation at different temperatures with G' .

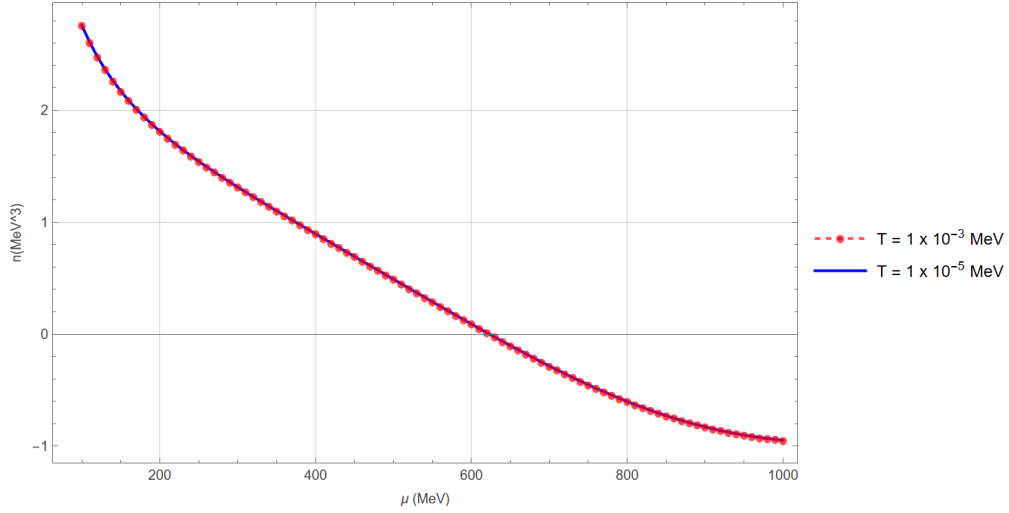


Figure 6: Calculation of the density n in the medium at low temperatures $T \approx 1 \times 10^{-3}$ MeV and 1×10^{-5} MeV with G'

axis. This suggests a progressive restoration of chiral symmetry without discontinuities. Now for G' the graph of Fig. 6 presents a crossover towards negative values at $\mu \approx 600 - 700$ MeV, denoting a more marked change in chiral cleavage, which is possibly greater over-clearance at intermediate densities and a more intense restoration at high densities. Although we do not analyze pairs of values $\mu - T$ where a jump in the values of the speed of sound is evident or a Gap Equation that shows a double solution, these indications of softness in the equation of state for the case G' in what would

be the vicinity of the CEP for very small T , indicate that we are in the vicinity of a first order and by refining the speed of sound with the complete expression at finite T we would notice the signal of the CEP in the expected values of the standard NJL results.

4 Discussion and Perspectives

The numerical results presented in Sec. 3 allow us to draw a coherent picture of how medium screening affects chiral symmetry restoration and the thermodynamic properties of dense quark matter within the NJL framework. The solution to the gap equation with a constant coupling G confirms the standard NJL behavior: the dynamical quark mass m decreases monotonically as the baryochemical potential μ increases beyond the constituent-quark scale, signaling the progressive restoration of chiral symmetry. The transition sharpens as the temperature is lowered, and for sufficiently small T it can become discontinuous, indicating a first-order phase transition [15, 12]. When screening is introduced through the medium-dependent coupling $G' = G m'/m$, the effective interaction is suppressed at large densities in a way that accelerates the restoration of the condensate. This behavior is physically motivated: in a dense medium the Debye screening of gluon exchanges weakens the four-fermion interaction, so the constituent mass should decrease more rapidly than the constant- G approximation suggests [23, 24, 25, 26]. Our parametrization captures this tendency in a minimal way and produces a qualitatively new feature: for intermediate chemical potentials ($\mu \approx 600$ – 700 MeV) the baryon number density n overshoots and crosses zero before settling into the high-density asymptotic regime, a behavior absent in the constant-coupling case. This crossing signals a more abrupt modification of the chiral order parameter and is a qualitative indicator of the proximity of a first-order transition and a CEP at very low temperatures.

The dependence of m on the seed mass m_0 shown in Fig. 2 further illustrates the role of the coupling: in the chiral limit ($m_0 \rightarrow 0$) a non-trivial solution is sustained up to a critical μ , while for larger m_0 the dynamical mass smoothly interpolates between the vacuum value and the perturbative regime. This pattern is consistent with standard NJL phenomenology [13, 14] and with Dyson–Schwinger studies of the dressed-quark propagator at finite density [23, 24].

The speed of sound c_s^2 is a particularly sensitive probe of the equation of state because it involves second derivatives of the thermodynamic potential and is therefore strongly amplified near phase transitions. In the present model, the exact expression (14) reduces, at leading order in the Sommerfeld

expansion ($T \rightarrow 0$), to $c_s^2 \approx n(\partial n/\partial \mu)^{-1}/\mu$, which we evaluate numerically and compare with the conformal value $c_s^2 = 1/3$.

For constant G , $c_s^2(\mu)$ rises smoothly from below $1/3$ toward the conformal limit, consistent with the expected behavior of a weakly interacting quark gas at large μ . This qualitative agreement with the perturbative QCD prediction $c_s^2 \rightarrow 1/3$ as $\alpha_s \rightarrow 0$ [27, 28] validates the thermodynamic consistency of our regularization scheme. The conformal limit is approached from below for the constant-coupling case, without exhibiting a peak exceeding $1/3$. This is in contrast with several recent analyses of dense matter in the context of neutron-star equations of state, where a peak above $1/3$ has been reported and associated with the onset of quark degrees of freedom or a crossover transition [17, 29, 16, 30]. The absence of such a peak in our model, for the parameter set considered, indicates that neither the standard NJL result nor the screened-coupling extension produce a super-conformal equation of state in the regime studied; the approach to $c_s^2 = 1/3$ is monotonic and from below.

When screening is activated through G' , the speed of sound retains the same asymptotic value but develops a more pronounced variation in the transitional region. The softer equation of state signaled by the negative excursion of $n(\mu)$ near $\mu \sim 600\text{--}700$ MeV leaves a clear imprint on c_s^2 : the function develops a dip or inflection in this range before recovering the conformal limit at high densities. This behavior is qualitatively analogous to the softening of c_s^2 near the QCD crossover observed in lattice calculations at $\mu = 0$ [4, 5] and in PNJL and Polyakov-extended quark-meson model studies at finite density [31, 32, 33]. A dip in c_s^2 at intermediate densities is also consistent with microscopic nuclear-matter calculations that incorporate repulsive short-range correlations and find a local minimum near the nuclear saturation density n_0 [29, 34]. Our results thus suggest that, even within the simplified NJL framework, screening effects generate a thermodynamic signature reminiscent of those transitions.

The combined evidence from the gap equation, the baryon density, and the speed of sound is consistent with the presence of a CEP in the vicinity of $\mu \approx 600\text{--}800$ MeV and $T \rightarrow 0$ when the screened coupling G' is employed. The negative excursion of n and the dip in c_s^2 are indirect indicators rather than definitive proofs, since a rigorous identification of the CEP requires the simultaneous divergence of the quark-number susceptibility $\chi_{\mu\mu}$ and a discontinuity in $m(\mu)$ at the same point. A precise determination of the CEP location is also sensitive to the specific parametrization of $G'(T, \mu)$, the regularization scheme, and the number of quark flavors considered, as has been documented in systematic NJL studies [15, 35, 13]. The standard NJL model without screening typically places the CEP at $\mu \approx 300\text{--}350$ MeV

and $T \approx 50\text{--}80$ MeV for two light flavors with Λ in the range 590–650 MeV [12, 15], while models incorporating Polyakov-loop dynamics tend to shift the CEP to somewhat larger μ [36, 37]. The present results, where screening pushes the relevant structure toward higher chemical potentials, are compatible with the expectation that in-medium weakening of the attractive scalar interaction delays chiral restoration. This is also consistent with functional renormalization group (FRG) studies that find a moderate shift of the CEP location when quantum and thermal fluctuations beyond the mean field are taken into account [32, 33, 38].

From an experimental standpoint, the speed of sound has been proposed as an observable that could encode signatures of a nearby phase transition or CEP through non-monotonic behavior in hadronic spectra and collective flow in heavy-ion collisions [39, 40, 41]. The sensitivity of c_s^2 to the specific form of $G'(T, \mu)$ shown in our analysis suggests that measurements at FAIR and NICA energies, which probe the baryon-rich region of the QCD phase diagram [9, 10, 42], could potentially discriminate between different screening scenarios. However, translating the behavior of c_s^2 as computed in the thermodynamic limit into experimentally accessible observables requires modeling of the dynamical evolution of the fireball and the freeze-out conditions, which lies beyond the scope of the present work.

The equation of state at low temperature and high density is directly relevant to the physics of neutron stars, where the core density may exceed several times the nuclear saturation density and the temperature is negligible on the QCD scale [43, 17]. In that context, a stiff equation of state (large c_s^2) is needed to support the observed two-solar-mass pulsars [44, 45, 46], while gravitational-wave observations place upper bounds on tidal deformabilities that disfavor equations of state that are too stiff at intermediate densities [47]. Our finding that the screened coupling produces a softer equation of state in the transitional region, while retaining the conformal limit at large μ , places the present model qualitatively in the range of behaviors compatible with compact-star constraints. A quantitative comparison would require extending the model to include strange quarks, diquark condensates, and a proper treatment of the nuclear–quark matter interface, as has been pursued in hybrid-star models [48, 49, 17].

Several simplifications of the present study warrant comment. First, the Hartree (mean-field) approximation omits mesonic fluctuations and hadronic degrees of freedom that can quantitatively modify the transition temperatures and chemical potentials, particularly near the CEP where the order parameter fluctuates strongly [32, 33]. Second, our choice of the screening ansatz $G' = G m'/m$ is physically motivated but phenomenological; a more systematic derivation of the in-medium coupling would require either a

Dyson–Schwinger calculation of the dressed gluon propagator at finite density [24, 50] or a running-coupling analysis in the spirit of the functional renormalization group [38, 51]. Third, the model does not include the vector channel, which is known to shift the CEP to larger μ and may even eliminate it entirely for sufficiently large vector coupling [15, 35, 52]. Fourth, we have worked in the isospin-symmetric limit; explicit isospin breaking, relevant to neutron-star matter, would modify the baryon-density equation and the susceptibilities. Finally, the Sommerfeld expansion employed here provides a reliable approximation for $T \ll \mu$ but breaks down in the intermediate-temperature regime where the two crossover temperatures are comparable. A full numerical treatment of the Fermi–Dirac integrals is necessary to map out the complete phase diagram, including the crossover region at $\mu < \mu_{\text{CEP}}$.

Future work will address these limitations by: (i) incorporating Polyakov-loop degrees of freedom to restore the interplay between confinement and chiral symmetry restoration [36, 37]; (ii) refining the parametrization of $G'(T, \mu)$ using Dyson–Schwinger or FRG input; (iii) extending the analysis to the three-flavor sector to include the strange quark and potential color-superconducting phases [53]; and (iv) computing the quark-number susceptibility and baryon-number fluctuations directly comparable with lattice QCD data in the crossover region [54, 55] and with freeze-out analyses of heavy-ion data [10, 9]. The results of the present paper provide a clear and physically motivated baseline for these extensions.

Acknowledgements

A. Raya and S.H.O. acknowledge support from SECIHTI and CIC-UMSNH (Mexico) under grants CBF-2025-G-1718 and 18371, respectively. S.H.O. acknowledges support from a SECIHTI (Mexico) postdoctoral project under grant EPA(3)-2022.

References

- [1] K. Fukushima and T. Hatsuda *Rept. Prog. Phys.*, vol. 74, p. 014001, 2011.
- [2] P. Braun-Munzinger and J. Wambach, “Colloquium: Phase diagram of strongly interacting matter,” *Rev. Mod. Phys.*, vol. 81, pp. 1031–1050, 2009.
- [3] Y. e. a. Aoki *Nature*, vol. 443, p. 675, 2006.

- [4] S. e. a. Borsanyi *Phys. Lett. B*, vol. 730, p. 99, 2014.
- [5] A. e. a. Bazavov *Phys. Rev. D*, vol. 85, p. 054503, 2012.
- [6] P. de Forcrand, “Simulating QCD at finite density,” *PoS*, vol. LAT2009, p. 010, 2010.
- [7] S. Muroya, A. Nakamura, C. Nonaka, and T. Takaishi, “Lattice QCD at finite density: An introductory review,” *Prog. Theor. Phys.*, vol. 110, pp. 615–668, 2003.
- [8] M. Stephanov *Prog. Theor. Phys. Suppl.*, vol. 153, p. 139, 2004.
- [9] X. Luo and N. Xu *Nucl. Sci. Tech.*, vol. 28, p. 112, 2017.
- [10] L. e. a. Adamczyk *Phys. Rev. Lett.*, vol. 112, p. 032302, 2014.
- [11] Y. Nambu and G. Jona-Lasinio *Phys. Rev.*, vol. 122, p. 345, 1961.
- [12] S. Klevansky *Rev. Mod. Phys.*, vol. 64, p. 649, 1992.
- [13] T. Hatsuda and T. Kunihiro *Phys. Rept.*, vol. 247, p. 221, 1994.
- [14] U. Vogl and W. Weise *Prog. Part. Nucl. Phys.*, vol. 27, p. 195, 1991.
- [15] M. Buballa *Phys. Rept.*, vol. 407, p. 205, 2005.
- [16] P. Bedaque and A. Steiner *Phys. Rev. Lett.*, vol. 114, p. 031103, 2015.
- [17] E. e. a. Annala *Nature Phys.*, vol. 16, p. 907, 2020.
- [18] Y. Nambu and G. Jona-Lasinio, “Dynamical model of elementary particles based on an analogy with superconductivity. i,” *Phys. Rev.*, vol. 122, pp. 345–358, Apr 1961.
- [19] J. Kapusta and C. Gale, *Finite Temperature Field Theory*. 2006.
- [20] N. Ashcroft and N. Mermin, *Solid State Physics*. 1976.
- [21] A. Fetter and J. Walecka, *Quantum Theory of Many-Particle Systems*. 1971.
- [22] A. Bazavov, H.-T. Ding, P. Hegde, O. Kaczmarek, F. Karsch, N. Karthik, E. Laermann, A. Lahiri, R. Larsen, S.-T. Li, S. Mukherjee, H. Ohno, P. Petreczky, H. Sandmeyer, C. Schmidt, S. Sharma, and P. Steinbrecher, “Chiral crossover in qcd at zero and non-zero chemical potentials,” *Physics Letters B*, vol. 795, pp. 15–21, 2019.

- [23] C. D. Roberts and A. G. Williams, “Dyson–Schwinger equations and their application to hadronic physics,” *Prog. Part. Nucl. Phys.*, vol. 33, pp. 477–575, 1994.
- [24] C. S. Fischer, “Infrared properties of QCD from Dyson–Schwinger equations,” *J. Phys. G*, vol. 32, pp. R253–R291, 2006.
- [25] R. e. a. Farias *Phys. Rev. C*, vol. 94, p. 065204, 2016.
- [26] R. L. S. Farias, V. S. Timoteo, S. S. Avancini, M. B. Pinto, and G. Krein, “Importance of asymptotic freedom for the pseudocritical temperature in magnetized quark matter,” *Eur. Phys. J. A*, vol. 53, p. 101, 2017.
- [27] E. S. Fraga, R. D. Pisarski, and J. Schaffner-Bielich, “Small, dense quark stars from perturbative QCD,” *Phys. Rev. D*, vol. 63, p. 121702(R), 2001.
- [28] A. Kurkela, P. Romatschke, and A. Vuorinen, “Cold quark matter,” *Phys. Rev. D*, vol. 81, p. 105021, 2010.
- [29] I. Tews, J. Carlson, S. Gandolfi, and S. Reddy, “Constraining the speed of sound inside neutron stars with chiral effective field theory interactions and observations,” *Astrophys. J.*, vol. 860, p. 149, 2018.
- [30] S. Furuseth and T. Husek, “Sound velocity peak and conformality in isospin QCD,” *Phys. Rev. D*, vol. 108, p. 054028, 2023.
- [31] K. Fukushima *Phys. Rev. D*, vol. 77, p. 114028, 2008.
- [32] B. Schaefer and M. Wagner *Phys. Rev. D*, vol. 79, p. 014018, 2007.
- [33] T. K. Herbst, J. M. Pawłowski, and B.-J. Schaefer, “The phase structure of the Polyakov–quark-meson model beyond mean field,” *Phys. Lett. B*, vol. 696, pp. 58–67, 2011.
- [34] K. Hebeler, J. M. Lattimer, C. J. Pethick, and A. Schwenk, “Equation of state and neutron star properties constrained by nuclear physics and observation,” *Astrophys. J.*, vol. 773, p. 11, 2013.
- [35] P. Costa, M. C. R. de Paoli, and C. A. de Sousa, “The QCD critical end point in the context of the Polyakov–Nambu–Jona-Lasinio model,” *Phys. Rev. D*, vol. 77, p. 096001, 2008.
- [36] K. Fukushima, “Chiral effective model with the Polyakov loop,” *Phys. Lett. B*, vol. 591, pp. 277–284, 2004.

- [37] C. Ratti, M. A. Thaler, and W. Weise, “Phases of QCD: Lattice thermodynamics and a field theoretical model,” *Phys. Rev. D*, vol. 73, p. 014019, 2006.
- [38] R.-A. Tripolt, J. Schaffner-Bielich, and J. Wambach, “Low-temperature behavior of the quark-meson model and the chiral condensate,” *Phys. Rev. D*, vol. 90, p. 034031, 2014.
- [39] D. H. Rischke, “Hydrodynamics and collective phenomena in heavy-ion collisions,” *Nucl. Phys. A*, vol. 610, pp. 88c–101c, 1996.
- [40] J. L. Nagle and W. A. Zajc, “Small system collectivity in relativistic hadronic and nuclear collisions,” *Annu. Rev. Nucl. Part. Sci.*, vol. 68, pp. 211–235, 2018.
- [41] P. Sorensen *et al.*, “Dense nuclear matter equation of state from heavy-ion collisions,” *Prog. Part. Nucl. Phys.*, vol. 134, p. 104080, 2024.
- [42] T. Ablyazimov *et al.*, “Challenges in QCD matter physics — the scientific programme of the Compressed Baryonic Matter experiment at FAIR,” *Eur. Phys. J. A*, vol. 53, p. 60, 2017.
- [43] F. Özel and P. Freire, “Masses, radii, and the equation of state of neutron stars,” *Annu. Rev. Astron. Astrophys.*, vol. 54, pp. 401–440, 2016.
- [44] P. B. Demorest, T. Pennucci, S. M. Ransom, M. S. E. Roberts, and J. W. T. Hessels, “A two-solar-mass neutron star measured using Shapiro delay,” *Nature*, vol. 467, pp. 1081–1083, 2010.
- [45] J. Antoniadis *et al.*, “A massive pulsar in a compact relativistic binary,” *Science*, vol. 340, p. 1233232, 2013.
- [46] E. Fonseca *et al.*, “Refined mass and geometric measurements of the high-mass PSR J0740+6620,” *Astrophys. J. Lett.*, vol. 915, p. L12, 2021.
- [47] B. P. Abbott *et al.*, “GW170817: Measurements of neutron star radii and equation of state,” *Phys. Rev. Lett.*, vol. 121, p. 161101, 2018.
- [48] M. Alford, M. Braby, M. Paris, and S. Reddy, “Hybrid stars that masquerade as neutron stars,” *Astrophys. J.*, vol. 629, pp. 969–978, 2005.
- [49] G. Baym, T. Hatsuda, T. Kojo, P. D. Powell, Y. Song, and T. Takatsuka, “From hadrons to quarks in neutron stars: a review,” *Rep. Prog. Phys.*, vol. 81, p. 056902, 2018.

- [50] C. D. Roberts and S. M. Schmidt, “Reflections upon the emergence of hadronic mass,” *Eur. Phys. J. ST*, vol. 120, pp. 167–188, 2000.
- [51] J. Braun, “Fermion interactions and universal behavior in strongly interacting theories,” *J. Phys. G*, vol. 39, p. 033001, 2012.
- [52] N. M. Bratovic, T. Hatsuda, and W. Weise, “Role of vector interaction and axial anomaly in the PNJL modeling of the QCD phase diagram,” *Phys. Lett. B*, vol. 719, pp. 131–135, 2013.
- [53] M. G. Alford, A. Schmitt, K. Rajagopal, and T. Schäfer, “Color superconductivity in dense quark matter,” *Rev. Mod. Phys.*, vol. 80, pp. 1455–1515, 2008.
- [54] S. Borsanyi *et al.*, “Fluctuations of conserved charges at finite temperature from lattice QCD,” *JHEP*, vol. 01, p. 138, 2012.
- [55] A. Bazavov *et al.*, “Skewness, kurtosis, and the fifth and sixth order cumulants of net baryon-number distributions from lattice QCD,” *Phys. Rev. D*, vol. 101, p. 074502, 2020.